JOURNAL OF Applied Polymer SCIENCE

Synthesis of epoxy curing agents containing different ring structures and properties investigation of the cured resins

Tingting Li,[1,2] Xiaoqing Liu,[1] Yanhua Jiang,[1] Songqi Ma,[1] Jin Zhu[1]

[1]Ningbo Institute of Material Technology and Engineering, Chinese Academy of Sciences, Ningbo, Zhejiang, 315201, People's Republic of China

[2]Nano Science and Technology Institute, University of Science and Technology of China, Suzhou, 215123, People's Republic of China

Correspondence to: X. Liu (E-mail:liuxq@nimte.ac.cn)

ABSTRACT: Two kinds of aliphatic epoxy curing agents containing ring structures were synthesized from rosin acid and isosorbide, respectively. They were cured with diglycidyl ether bisphenol A (DER331) and the ultimate propertied of the cured resins were investigated. For comparison, the petroleum-based curing agent containing planar benzene ring was synthesized from terephthalic acid. The chemical structures of the synthesized curing agents were identified by Fourier transform-infrared and H-nuclear magnetic resonance. The ultimate properties of the cured epoxy resins were investigated by thermogravimetric analysis and dynamic mechanical analysis. Especially, the effects of ring structure on their shape memory properties were studied in terms of shape fixity, shape recovery, and shape recovery time. © 2016 Wiley Periodicals, Inc. J. Appl. Polym. Sci. **2016**, *133*, 44219.

KEYWORDS: bio-based polymers; thermosets; mechanical properties

Received 18 April 2016; accepted 21 July 2016
DOI: 10.1002/app.44219

INTRODUCTION

Shape memory polymers (SMPs) are stimuli-sensitive materials that can be deformed and fixed in a temporary shape and then recover the original shape when exposed to a suitable stimulus, such as electric field,[1] temperature,[2] moisture,[3] light,[4] pH,[5] or magnetic field.[6] They have been used extensively as sensors, smart adhesives, actuators and self-deployable medical devices. Thermosetting resins are important members of SMPs due to their good thermal and chemical stability,[7] high shape recovery stress, and high shape fixity ratio. Up to now, a large quantity of epoxy resins with good shape memory properties has been reported. And diglycidyl ether of bisphenol A (DGEBA) is the dominant precursor. For example, Agustina[8] reported an epoxy network based on DGEBA showing relatively high tensile strains, good values of shape fixity, and shape recovery. Ingrid[9] prepared a series of shape memory epoxies possessing high thermal–mechanical endurance and excellent shape memory performances. Wu *et al.*[10] discovered a new type of epoxy resin, diglycidyl ether of 9,9-bis [4-(2-hydroxyethoxy) phenyl] fluorine (DGEBEF) and the DGEBEF/DDS system exhibited excellent shape memory properties.

In recent years, with diminishing petroleum resources and aggravating environmental pollution, scientists and researchers have been increasingly concerned about environmental friendly and renewable materials. Bio-based polymers as environment-friendly materials have more significant effect on our life and scientific research.[11] Until now, a lot of renewable feedstocks, such as rosin acid,[12,13] isosorbide,[14,15] itaconic acid,[16] and many other natural products,[17–23] have been used to prepare bio-based thermosetting resins. For instance, a series of biobased epoxies derived from rosin acid have been reported and their thermal or mechanical properties were better or similar to their petroleum-based counterparts.[12,13] Ma *et al.*[21] synthesized the epoxies from itaconic acid (IA) and the multiple functional groups ensured them good mechanical properties. Takashi *et al.*[22] reported the synthesis of plant oil-based shape memory materials from epoxidized soybean oil (ESO) and polycaprolactone (PCL). The polyESO/PCLs exhibited excellent shape memory properties, and the strain fixity depended on the feed ratio of ESO and PCL.

As we know, epoxy resin is mainly composed of two parts, epoxy compound and curing agent. The structure of curing agent has significant effect on the properties of cured epoxy resins. Therefore, it is possible for us to manipulate their ultimate properties by varying curing agents.[24] Recently, the compounds containing non-planar ring structures have been employed for the polymers with good shape memory properties and satisfied results have been achieved. For example, the hydrogen

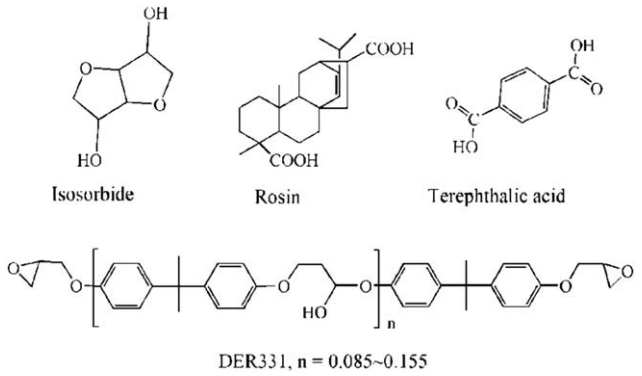

Scheme 1. Chemical structures of isosorbide, rosin acid, terephthalic acid, and DER331.

phenanthrene ring in rosin acid was used to increase the polyurethanes' recoverable strain and shape recovery ratio dramatically.[25] The epoxy derived from isosorbide showed good shape fixity, good shape recovery, and satisfied thermal stability.[26] And the reason was supposed to be corresponding to the conformational transition of the non-planar ring structure during the thermal treatment process. In this article, we exploited the chemical structures of biobased rosin acid and isosorbide to synthesize curing agents containing different ring structures [aminated acrylicpimaric acid (RSR) and aminated isosorbide (ISR), as shown in Scheme 1]. For comparison, the curing agent derived from petroleum-based terephthalic acid (TAR, Scheme 1) was also used here as the reference and cured with the same epoxy DER331. The ultimate properties of the cured epoxy resins were investigated. Especially, the effects of ring structure on their shape memory properties were studied in terms of shape fixity, shape recovery, and shape recovery time. The objective of this work is to develop the biobased epoxy with shape memory properties.

MATERIALS

Rosin acid (RA, with the purity of 75%), allyl bromide (98%), hydroquinone (99%), benzoin dimethyl ether (DMPA), acrylic acid (99%), and cysteamine hydrochloride were all obtained from Aldrich, China. Acetone (99%), petroleum ether (50–90 °C), sodium hydroxide (99%), potassium carbonate (99%), diethyl ether (99%), anhydrous sodium carbonate (Na_2CO_3), magnesium sulfate ($MgSO_4$), dichloromethane (CH_2Cl_2, 99%), and terephthalic acid (TPA) were brought from Sinopharm Chemical Reagent Co., Ltd., China. Isosorbide (99%) was provided by RiZhao LeDeShi Chemical Co., Ltd., China. Diglycidyl ether of bisphenol A, DER-331 (DGEBA) with an epoxy equivalent weight of 182–192 was bought from Dow chemical Inc. (China). All the chemicals were used as received.

CHARACTERIZATION

The Fourier transform infrared (FT-IR) spectrum was recorded with Nicolet 6700 FT-IR, scanning from 4000 to 400 cm^{-1}. NMR was performed on a Bruker 400 MHz AVANCE III spectrometer with the solvent of $CDCl_3$. Chemical shifts of ^1H NMR and ^{13}C NMR were referenced to the peak of residual $CHCl_3$ at 7.26 and 77 ppm, respectively. The differential scanning calorimetry (DSC) measurement was conducted on a Mettler-Toledo TGA/DSC1 under a nitrogen atmosphere. The samples weighted about 7 mg and the test was conducted from 25 to 200 °C with heating rates of 5, 10, 15, 20 °C/min, respectively. The thermogravimetric analyses (TGA) measurement was performed on a Mettler-Toledo TGA/DSC1 thermogravimetric analyzer (METTLER TOLEDO, Switzerland) with high purity nitrogen at a scanning rate of 10 °C/min from 50 to 800 °C. Dynamic mechanical analysis (DMA) was performed on Mettler Toledo DMA/SDTA 861e using a tensile mode at a frequency of 1 Hz. All the samples with the dimension of 2.5 mm × 4.0 mm × 1.2 mm were tested from 25 to 180 °C at a rate of 2 °C/min. Rectangular specimens with the dimension of 75 mm × 7.1 mm × 1.6 mm were used to evaluate shape memory properties of the epoxy resin. The shape memory test was carried out according to the following steps:[27] (1) The specimens were heated to a predetermined temperature ($T_g + 30$ °C); (2) The specimens were bent into "U shape" (the maximum angle of bending was the angle θ_{max}); (3) the U-shaped specimens were cooled to room temperature and the external force was removed after several minutes to fix the temporary shape (the bending angle of the fixed sample became the angle θ_{fixed}); (4) The U-shaped specimens were reheated to $T_g + 30$ °C to recover its original shape (the deformation angle at the original state was θ_{final}) and the shape recovery process was observed. The shape fixity (R_f) and shape recovery (R_r) were calculated using the following eqs. (1) and (2):

$$R_f = [\theta_{fixed}/\theta_{max}] \times 100\% \quad (1)$$

$$R_r = [(\theta_{fixed} - \theta_{final})/\theta_{max}] \times 100\% \quad (2)$$

where the angle θ_{max} was the maximum angle of bending, the angle θ_{fixed} was the initial deformation angle of the fixed sample, and the angle θ_{final} was the deformation angle at the original state.

SYNTHESIS OF ACRYLICPIMARIC ACID (APA)

APA was synthesized according to the procedures described in our previous article.[13] Rosin acid (30.2 g, 0.10 mol), acrylic acid (8.8 g, 0.12 mol), and hydroquinone (0.2 g, 0.0012 mol) were added into a 500 mL three-neck flask equipped with magnetic stirrer and reflux condenser under N_2 atmosphere. The mixture was stirred at 140 °C for 30 min, 160 °C for 30 min, and 180 °C for 9 h under the protection of nitrogen. After that, the reaction was stopped and cooled to room temperature. The mixture was dissolved in anhydrous ether and precipitated in excess petroleum ether. The precipitate was collected by filtration and washed three times with deionized water. The crude product was recrystallized from acetone to obtain the pure APA which is a white, solid, and granular material 17.4 g (yield: 56%):

^1H-NMR (400 MHz, $CDCl_3$, δ ppm); 5.4 (s, H, =CH— in rosin ring), 2.5 (s, H, —CH—), 2.2–2.4 (m, 2H, —CH—CH—), 0.5–2.0 (m, 28H, protons in rosin ring, —C—CH—), ^{13}C-NMR (CD_3Cl, δ ppm): 185, 183, 144, 127, 55, 52, 46, 44, 39, 38, 35, FT-IR (cm^{-1}); 2943, 2870, 1693, 1461, 1275, 1153.

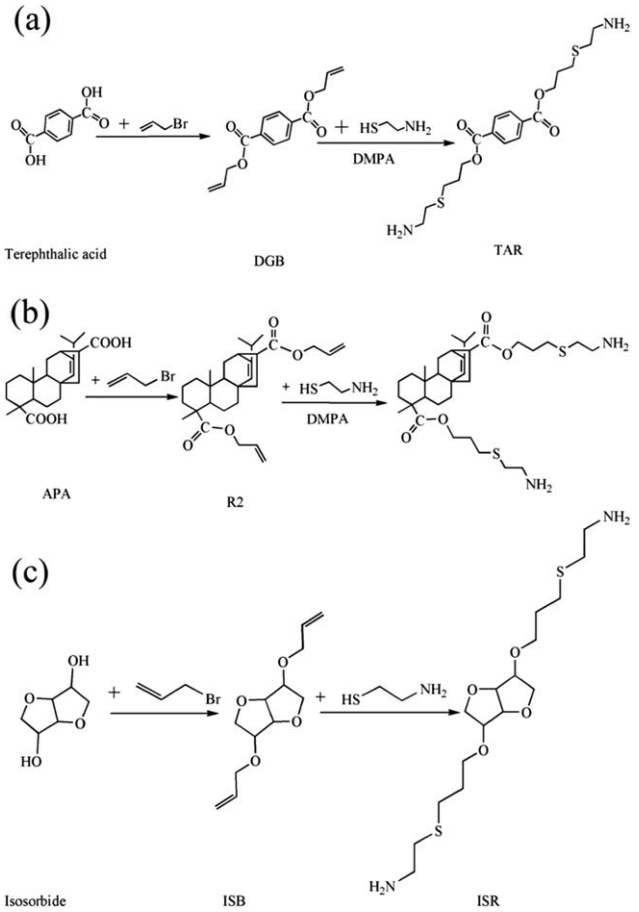

Scheme 2. Synthesis procedure of TAR from TPA (a), RSR from Rosin acid (b), and ISR from isosorbide (c).

SYNTHESIS OF DIVINYL ACRYLICPIMARIC ACID (R2)

APA (14.4 g, 0.039 mol), K_2CO_3 (10.4 g, 0.075 mol), and 30 mL of acetone were added into a 250 mL three-necked flask equipped with a reflux condenser and a thermometer. The mixture was heated to 70 °C and a solution of allyl bromide (18.2 g, 0.15 mol) dissolved in 30 mL of acetone was added dropwise. After the reaction of the flask was maintained at 70 °C for another 15 h, it was cooled to room temperature before washing with CH_2Cl_2. The organic phase was collected by extraction and washed three times with deionized water before removing solvents with a rotary evaporator at 60 °C. At last a yellowy liquid product weighing 13.6 g was obtained (yield: 81%). The reaction is shown in Scheme 2(b):

^{1}H-NMR (400 MHz, $CDCl_3$, δ ppm); 5.9 (m, 2H, ═CH—), 5.2–5.3 (m, 5H, ═CH— in rosin ring, ═CH_2), 4.6 (s, 2H, O—CH—),4.5 (s, 2H, O—CH—), 2.5 (s, H, —CH—), 2.2–2.4 (m, 2H, —CH—CH—), 0.5–2.0 (m, 28H, protons in rosin ring, —C—CH—), ^{13}C-NMR (CD_3Cl, δ ppm); 178, 174, 148, 131, 123, 117, 65, 55,53, 49, 47, 40, 36, 35, 33, 28, 22, 21, 17, FT-IR (cm^{-1}); 2940, 2870, 1724, 1650, 1146, 927, 990.

SYNTHESIS OF AMINATED R2 (RSR)

R2 (11.00 g, 0.024 mol), cysteamine hydrochloride (5.61 g, 0.05 mol), and 0.1 equivalent of DMPA were dissolved in 70 mL mixture of 1,4-dioxane/ethanol (70/30 v/v). After the UV-irradiation (power: 36 W, wavelength: 365 nm) was carried out for 4 h, the reaction was stopped. Then ethanol was removed with a rotary evaporator at 40 °C and organic phase was washed with Na_2CO_3 saturated solution. Finally, the organic phase was collected by extraction and washed three times with deionized water before removing solvents with a rotary evaporator at 70 °C. A yellow-brown product weighing 8.46 g was obtained (yield: 58%). The reaction is shown in Scheme 2(b):

^{1}H-NMR (400 MHz, $CDCl_3$, δ ppm); 5.3 (s, H, ═CH— in rosin ring), 4.2 (m, 2H, —O—CH_2—), 4.0 (m, 2H, —O—CH_2—), 2.8 (m, 4H, N—CH_2—), 2.5–2.6 (m, 8H, —CH_2—S—CH_2—), 2.2–2.4 (m, 2H, —CH—CH—), 2.0 (m, 4H, —CH_2—), 0.5–1.9 (m, 32H,protons in rosin ring, —C—CH—, —NH_2), ^{13}C-NMR (CD_3Cl, δ ppm); 180, 175, 149, 124, 63, 55, 52, 49, 47, 41, 39, 38, 37, 36, 33, 29, 28, 21, 20, 16, 17, FT-IR (cm^{-1}); 3345, 2938, 1716, 1646, 1153.

SYNTHESIS OF DIVINYL TEREPHTHALIC ACID (DGB)

TPA (20 g, 0.12 mol), N,N-dimethylformamide (DMF, 120 mL), allyl bromide (80 g, 0.67 mol), 80 mL of acetone, and triethylamine (58.4 g, 0.58 mol) were put into a 500 mL round-bottomed flask equipped with thermometer, magnetic stirrer, and reflux condenser. The mixture was stirred at 65 °C for 24 h after the solid was dissolved completely in the solution. Then the reaction was stopped and the precipitate was removed by filtration. After that, the acetone, unreacted allyl bromide and triethylamine in the solution were removed using a rotary evaporator. Next, the remained organic phase was washed by deionized water four times after it was diluted with CH_2Cl_2. After drying the solution with $MgSO_4$, the solvents were removed with a rotary evaporator at 60 °C to obtain a yellow liquid product weighting 25.7 g (yield: 87%). The reaction is shown in Scheme 2(a):

^{1}H-NMR (400 MHz, $CDCl_3$, δ ppm); 8.1 (s, 4H, aromatic protons), 6.0 (m, 2H, —CH═), 5.3–5.5 (m, 4H, ═CH_2), 4.6 (d, 4H, —O—CH_2—), ^{13}C-NMR (CD_3Cl, δ, ppm); 166, 135, 133, 130, 119, 65, FT-IR (cm^{-1}); 3084, 2981, 2940, 1731, 1652, 1446, 1361, 1270, 1103, 971, 934, 733.

SYNTHESIS OF AMINATED TAR

DGB (5.05 g, 0.02 mol), cysteamine hydrochloride (4.75 g, 0.042 mol), and 0.1 equivalent of DMPA were dissolved in 40 mL of cosolvents: 1,4-dioxane/ethanol (70/30 v/v). After the UV-irradiation (36 W, 365 nm) was carried out for 4 h, the reaction was stopped. Then ethanol was evaporated by a rotary evaporator and organic phase was washed with Na_2CO_3 saturated solution. The organic phase was collected by extraction and washed three times with deionized water before removing solvents with a rotary evaporator at 70 °C. At last, a white solid product weighing 5.50 g was obtained (yield: 67%). The reaction is shown in Scheme 2(a):

^{1}H-NMR (400 MHz, $CDCl_3$, δ ppm); 8.1 (s, 4H, aromatic protons), 4.5 (t, 4H, —O—CH_2—), 2.9 (t, 4H, N—CH_2—), 2.6–2.7 (m, 8H, —CH_2—S—CH_2), 2.1 (m, 4H, —CH_2—),1.5 (s, 4H, —NH_2), ^{13}C-NMR (CD_3Cl, δ ppm); 166, 135, 130, 64, 41, 36, 28, 29, FT-IR (cm^{-1}); 3349, 2951, 2915, 1705, 1640, 1559, 1466, 1375, 1276, 1107, 731.

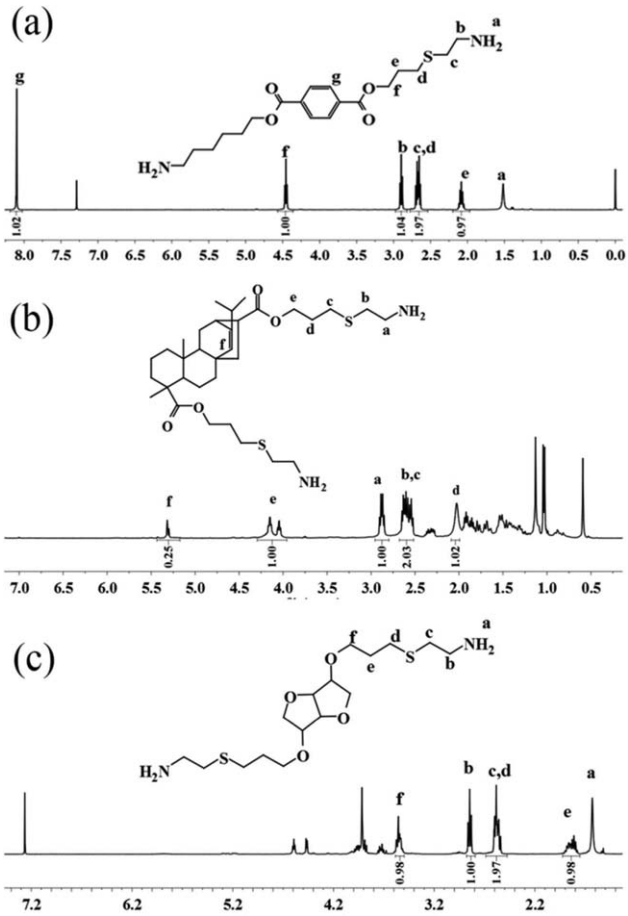

Figure 1. ^{1}H NMR of TAR (a), RSR (b), and ISR (c).

SYNTHESIS OF ISOSORBIDE DIALLYL ETHER (ISB)

Isosorbide (14.61 g, 0.1 mol) with allyl bromide (26.62 g, 0.22 mol) were put into a 250 mL three-necked flask equipped with magnetic stirrer, reflux condenser, and thermometer. Sodium hydroxide (8.8 g, 0.22 mol) dissolved in 25 mL deionized water was added dropwise. After stirring at 65 °C for 7 h, the reaction was stopped and cooled to room temperature. Then the solution was washed by deionized water three times after it was diluted with CH_2Cl_2. The organic phase was collected by extraction and dried with $MgSO_4$ before CH_2Cl_2 was removed with a rotary evaporator at 60 °C. At last, a yellow liquid product weighing 21.0 g was obtained (yield: 85%). The reaction is shown in Scheme 2(c):

^{1}H-NMR(400 MHz,$CDCl_3$, δ ppm); 5.9 (m, 2H, CH═), 5.3 (d, 2H, ═CH_2), 5.2 (d, 2H, ═CH_2), 4.6 (t, H, —O—CH—), 4.5 (d, H, —O—CH—), 3.5–4.2 (m,10H, —O—CH_2—, —O—CH—CH_2—), ^{13}C-NMR (CD_3Cl, δ ppm);134, 117, 87, 84, 80, 79, 73, 72, 71, 70, FT-IR (cm^{-1}); 3076, 2937, 2870, 1644, 1458, 1270, 1120, 998, 927.

SYNTHESIS OF AMINATED ISR

ISB (10.05 g, 0.045 mol), cysteamine hydrochloride (10.39 g, 0.092 mol) together with 0.1 equivalent of AIBN were dissolved in 80 mL of cosolvents: 1,4-dioxane/ethanol (70/30 v/v). The reaction was conducted at 85 °C for 24 h and then it was cooled to room temperature before the ethanol was evaporated by a rotary evaporator. After the solution was washed with Na_2CO_3 saturated solution, the organic phase was collected by extraction. Then it was washed three times with distilled water again and dried with $MgSO_4$ before the solvent was removed with a rotary evaporator at 60 °C. At last, a yellow liquid product weighing 10.36 g was obtained (yield: 61%). The reaction is shown in Scheme 2(c):

^{1}H-NMR (400 MHz, $CDCl_3$, δ ppm); 4.6 (t, H, —O—CH—), 4.5 (d, H, O—CH—), 3.7–4.2 (m, 6H, —O—CH—CH_2—), 3.6 (m, 4H, —O—CH_2—), 2.8 (m, 4H, —CH_2—), 2.6 (m, 8H, —CH_2—S—CH_2—), 1.8 (m, 4H, —CH_2—), 1.6 (s, 4H, —NH_2), ^{13}C-NMR (CD_3Cl, δ ppm); 87, 84, 80, 81, 77, 76, 73, 69, 68, 66, 42, 36, 29, 27, FT-IR (cm^{-1}); 3349, 2921, 2869, 1569, 1474, 1315, 1081.

CURING PROCEDURE

Epoxy resin (DER 331) was cured with curing agent (ISR, RSR, or TAR) in a 1:1 equivalent ratio. An appropriate amount of

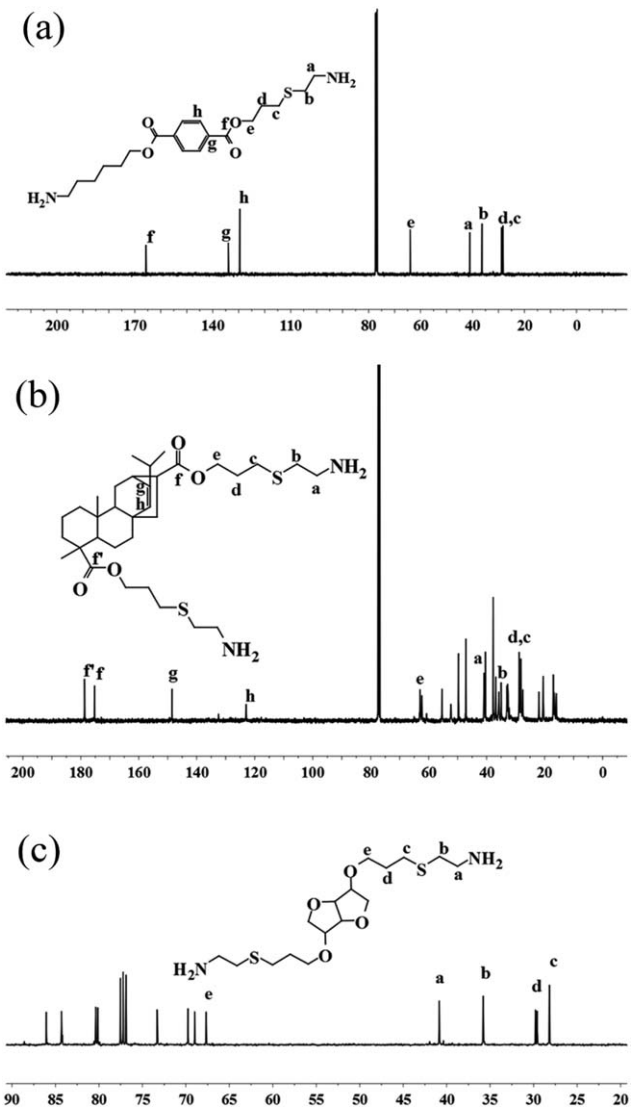

Figure 2. ^{13}C NMR of TAR (a), RSR (b), and ISR (c).

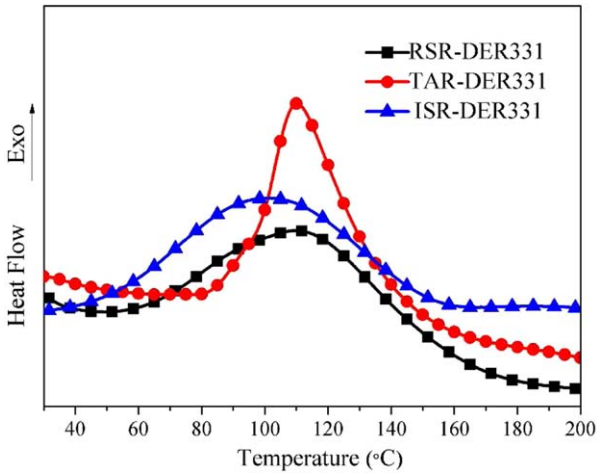

Figure 3. DSC thermograms of RSR/DER331, TAR/DER331, and ISR/DER331 combinations at a heating rate of 5 °C/min. [Color figure can be viewed in the online issue, which is available at wileyonlinelibrary.com.]

dichloromethane was added to dissolve the curing agent and epoxy before it was stirred for 30 min at room temperature to form a homogeneous system. The mixture was transferred into a vacuum oven at 50 °C for 1 h to get rid of the solvent and then poured into a stainless steel mold. The curing reaction was conducted at 80 °C for 2 h, 100 °C for 2 h, and 140 °C for 4 h to achieve fully cured resins. All the samples were cured under the same conditions and removed from the mold for dynamic mechanical analysis, thermal, and shape memory properties tests.

RESULTS AND DISCUSSION

Characterization of ISR, TAR, and RSR

The synthetic routes and chemical structures of RSR, ISR and TAR are shown in Scheme 2. Obviously, they were all synthesized via a two-step reaction: (1) Grafting the vinyl group to carboxylic group so as to introduce the double bonds; (2) Converting double bonds into amine groups via thiol-ene reaction. The detailed procedures were described in the experimental section and it was notable that all the reactions were conducted under relatively mild conditions.

Figure 1 is the ^{1}H-NMR spectrum and the peak identification for TAR, RSR, and ISR. In Figure 1(a), the peak at 8.2 ppm was assigned to the protons (H_g) attached on benzene ring. The H_f in —OCH_2— showed characteristic peaks at 4.5 ppm and the peaks appeared at 2.7 ppm and 2.9 ppm stood for H_c, H_d, and H_b, respectively. In addition, the integrated area of the characteristic signals for H_g, H_f, H_b, and H_c could be expressed by the equation of H_g:H_f:H_c:H_d =1:1:1:1, which was in good consistent with the theoretical value, which proved that TAR had two thioethylamine groups. In Figure 1(b,c), the characteristic peaks were all assigned to the protons accordingly and their chemical shifts data were very much in line with the theoretical ones. In order to further identify their structures, the ^{13}C NMR spectra of TAR, ISR and RSR were also displayed in Figure 2. In Figure 2(a), The C_e in —OCH_2— showed characteristic peaks at 64 ppm and the peaks appeared at 41, 36, 29, and 28 ppm stood for C_a, C_b, C_d, and C_c, respectively. In Figure 2(b,c), the characteristic peaks were all assigned to the carbon atoms accordingly and their chemical shifts data were very much in line with the theoretical ones. Combined with the FT-IR information listed in the experimental section, it could be concluded that the result of the synthesis was indeed as expected.

Curing Behavior of Different Cured Systems

Figure 3 shows the DSC curves of RSR/DER331, TAR/DER331 and ISR/DER331 combination at a heating rate of 5 °C/min. Apparently, each curve displayed a single exothermic peak corresponding to the ring opening reaction between epoxide

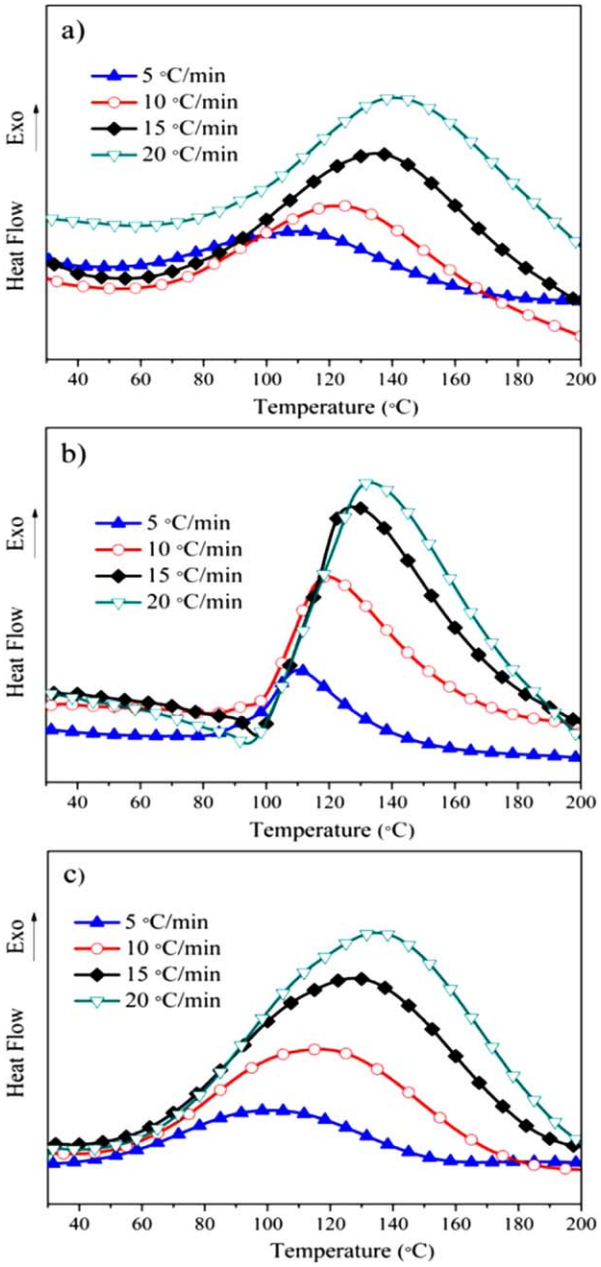

Figure 4. Typical DSC thermograms of (a) RSR/DER331, (b) TAR/DER331, and (c) ISR/DER331 combinations at different heating rate of 5, 10, 15, and 20 °C/min. [Color figure can be viewed in the online issue, which is available at wileyonlinelibrary.com.]

Table I. Activation Energy (E_a) for the Different Cured Combinations

Samples	Heating rates (°C/min)	Peak temp. (°C)	E_a (kJ/mol) Kissinger	Standard deviation	Ozawa	Standard deviation
ISR/DER331	5	100.7	49.3	4.8	53.4	5.2
	10	116.7				
	15	172.2				
	20	132.8				
TAR/DER331	5	109.5	64.8	3.6	67.8	3.4
	10	119.5				
	15	127.5				
	20	133				
RSR/DER331	5	111.1	61.5	2.6	64.8	3.1
	10	123.8				
	15	133.7				
	20	139.5				

groups of DGR331 with the corresponding amino groups of RSR, TAR, and ISR, respectively. Under the same curing condition, the peak temperature is usually taken as an indicator to evaluate the reactivity of the curing reactions.[28] The lower the peak temperature is, the higher the reactivity is. Obviously, the peak temperature of ISR/DER331 was lower than those of TAR/DER331 and RSR/DER331. And the TAR/DER331 and RSR/DER331 system showed the exothermic peak almost at the same temperature. These results indicated that the reactivity of ISR/DER331 system was higher than those of TAR/DER331 and RSR/DER331.

In order to compare their curing reactivity quantitatively, both Kissinger's[29] and Ozawa's[30] methods were employed here to estimate the activation energy of the different curing systems. Figure 4 shows the DSC curves of the different cured combination at different heating rates. It was easy to notice that all the systems showed a single exothermic peak, and the peak temperature was increased along with the increasing heating rate. The peak temperatures for different systems at different heating rates were listed in Table I. Based on Kissinger's theory, the activation energy could be estimated by the following eq. (3):

$$-\ln\left(q/T_p^2\right)=E_a/RT_p-\ln(AR/E_a) \quad (3)$$

where T_p is the exothermic peak temperature, q is the heating rate, E_a is the activation energy of the different cured combinations, R is the gas constant (8.314 J/mol/K), and A is the pre-exponential factor. E_a value could be obtained from the slope of linear fitting plots of $-\ln(q/T_p^2)$ versus $1/T_p$ Ozawa's method can be shown by eq. (4):

$$\ln q=-1.052\times E_a/RT_p+\ln(AE_a/R)-\ln F(\chi)-5.331 \quad (4)$$

where $F(\chi)$ is a conversion dependent term. The E_a value could also be determined from the slope of linear fitting plots of ln q versus $1/T_p$. Figure 5 shows the plots of $-\ln(q/T_p^2)$ versus $1/T_p$ based on Kissinger's equation (a) as well as ln q versus $1/T_p$

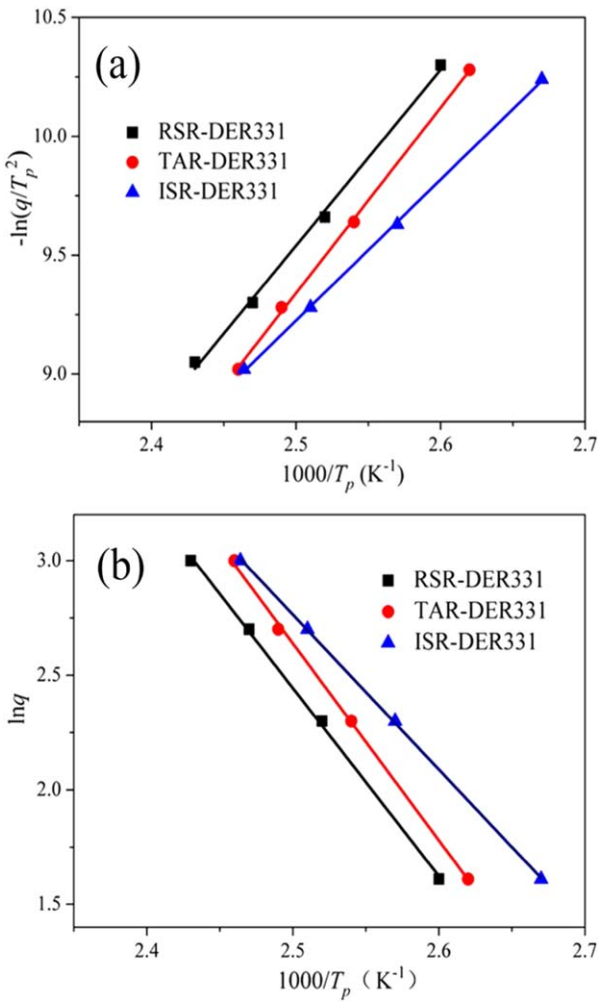

Figure 5. Linear plot of (a) $-\ln(q/T_p^2)$ versus $1/T_p$ based on Kissinger's equation and (b) ln q versus $1/T_p$ based on Ozawa's theory. [Color figure can be viewed in the online issue, which is available at wileyonlinelibrary.com.]

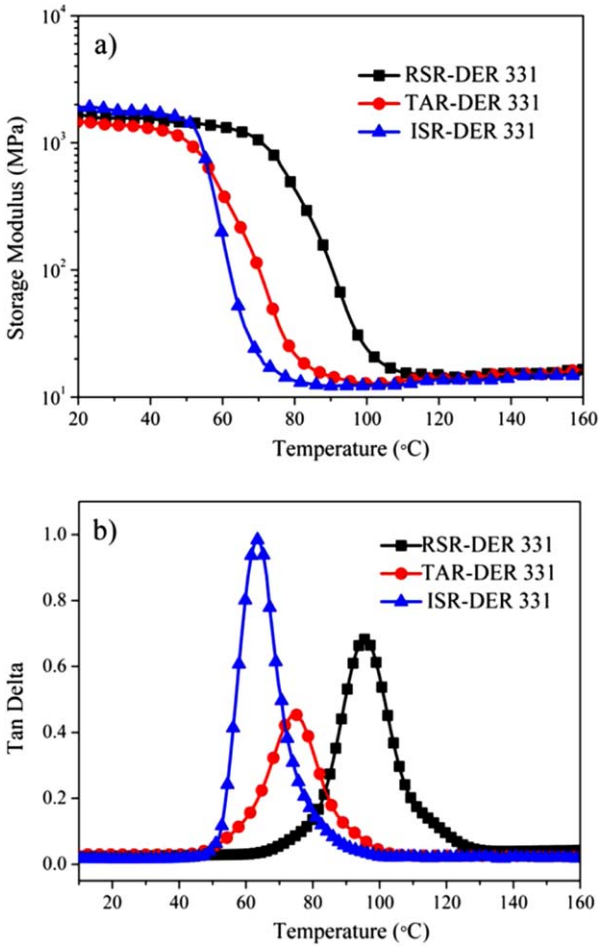

Figure 6. DMA curves of storage modulus-temperature (a) and tan α-temperature for the cured combinations. [Color figure can be viewed in the online issue, which is available at wileyonlinelibrary.com.]

based on Ozawa's equation (b) for RSR/DER331, TAR/DER331, and ISR/DER331 combinations. The E_a values of the different cured combinations were shown in Table I and Figure 6. In reactivity, ISR/DER331 is higher than those of RSR/DER331 and TAR/DER331.

Dynamic Mechanical Properties of the Cured Epoxy Resins

The dynamic mechanical properties of the different cured systems were investigated by DMA. Figure 6 is the DMA plots of DER331 cured with RSR, ISR, and TAR. Generally speaking, when the storage modulus of cured resin demonstrated two orders of magnitude difference before and after passing the glass transition temperature, it has the potential to be used as shape memory material.31 Figure 6(a) shows that all the cured systems demonstrated more than two orders of magnitude decrease in storage modulus when passed the glass transition temperature, which indicated that they could be used as SMPs. Figure 6(b) shows the loss tangent (tan α) for the different cured combinations as a function of temperature. Obviously, the T_g of RSR/DER331 (96 °C) was much higher than those of TAR/DER331 (75 °C) and ISR/DER331 (64 °C). The reason might be corresponded to the steric hindrance of rosin ring structure, which led to lower chain mobility so as to result in an elevated T_g.

Shape Memory Properties

To investigate the shape memory properties of these, rectangular specimens were tested at $T_g + 30$ °C using a U-type shape memory test. Figure 7 shows shape recovery times and shape memory recycle of these at $T_g + 30$ °C and the data for their shape memory properties are listed in Table II. According to the results, the shape fixed ratio (R_f) and recovery ratio (R_r) are almost 100%, which means good shape memory performance.32 Figure 7(a) reveals the relationship between recovering angle and recovering time of these at $T_g + 30$ °C. The maximum of shape recovery rates was observed in TAR/DER331 and the minimum is done in RSR/DER331. The shape recovery rates in ISR/DER331 did not appear to be much different from TAR/DER331. One possible reason is to the movements of chain structures. Rosin acid and isosorbide contain alicyclic non-planar ring structures which might play a cushioned function in the movement of chain. The movement of planar aromatic ring structure is easier than non-planar alicyclic structures. The shape recovery time in TAR/DER331 would be least. Meanwhile, replacing the two fused tetrahydrofuran ring structures with the

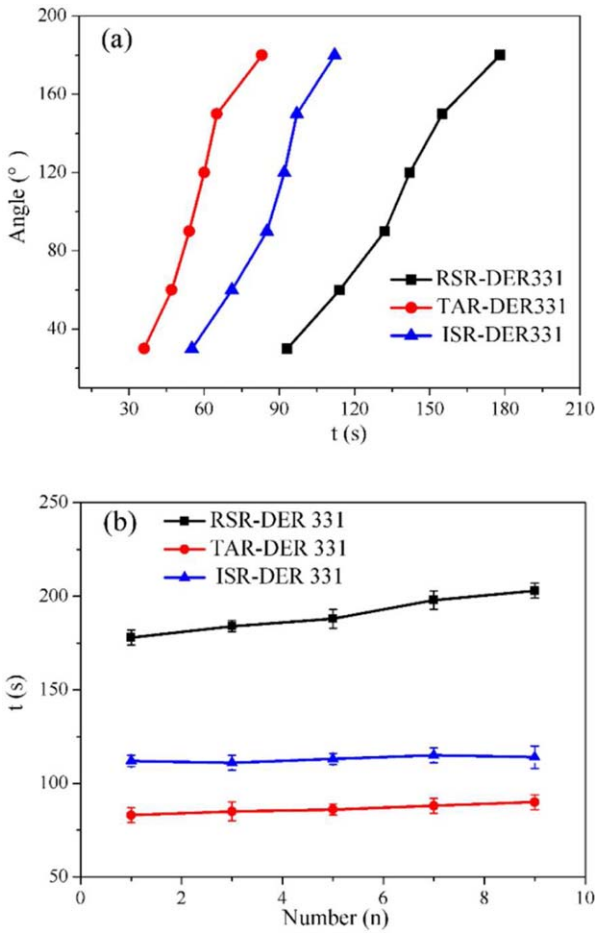

Figure 7. Shape recovery time of the cured combinations (a) and shape memory recycle of cured combinations (b). [Color figure can be viewed in the online issue, which is available at wileyonlinelibrary.com.]

Table II. Shape Fixity, Shape Recovery, and Shape Recovery Time of the Cured Combinations

Samples	R_f	R_r	T_{d5} (°C)	T_{d30} (°C)	T_s (°C)
IRS/DER331	98.8	98.9	306	344	161
TAR/DER331	98.3	97.2	310	346	162
RSR/DER331	98.5	96.9	314	353	165

rosin ring structure increases the chain rigidity of the material. Therefore, the shape recovery process in RSR/DER331 would be slowest. Figure 7(a) shows the relationship between recovering angle and recovering time of the shape memory effects at $T_g + 30$ °C and reveals that the recovery rate decreases at the last stage from 150° to 180°. This can be explained by the reason that the main stored strain energy has been released at the earlier stages, resulting in the relatively slow recovery rate of the samples at the last stage.[31] These shape memory properties of these are demonstrated in Figure 7. Starting from the original rectangular shapes, the samples can be deformed into different shapes through bending. These deformed temporary shapes (C shapes) were cooled down at room temperature for fixing the shape. Subsequent the samples were reheated in a $T_g + 30$ °C oven allowed complete recovery of the original rectangular shapes. The original rectangular specimens (40 × 4 × 1 mm^3) were used to demonstrate the shape recovery process of the different cured systems. Figure 8 shows the order of recovery rates: TAR/DER331> ISR/DER331 > RSR/DER331. Figure 7(b) shows the shape memory recycle of different cured systems and it reveals that the shape recovery times are almost not changed with the increasing cycle number. This indicated the good shape memory cyclic performance.

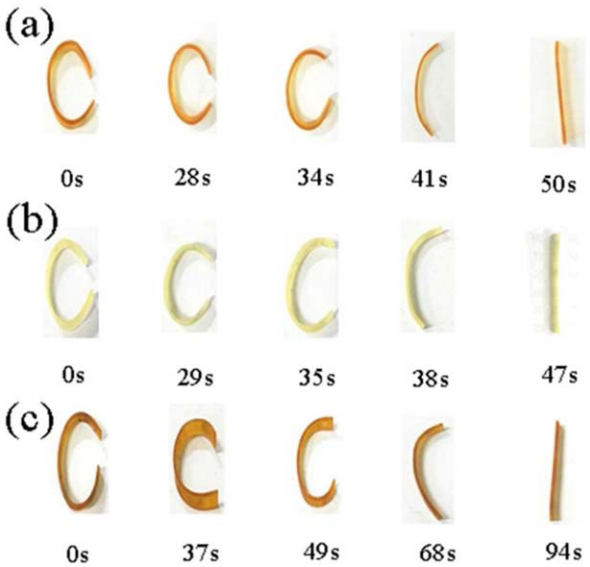

Figure 8. The shape recovery process of cured combinations in T_g +30 °C oven. (a) Presents time-resolved photographs of ISR/DER331 as a function of time at 94 °C. (b) Indicates time-resolved photographs of TAR/DER331 at 105 °C. (c) Shows time-resolved photographs of RSR/DER331 at 126 °C. [Color figure can be viewed in the online issue, which is available at wileyonlinelibrary.com.]

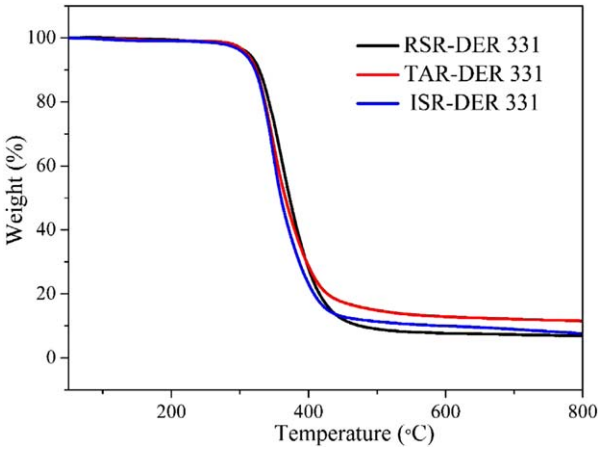

Figure 9. TGA curves of different cured combinations. [Color figure can be viewed in the online issue, which is available at wileyonlinelibrary.com.]

Thermal Degradation Behavior of the Cured Epoxy Resins

Figure 9 shows the TGA curves for DER331 cured with RSR, ISR and TAR, respectively. The values of the degradation temperature for 5% weight loss (T_{d5}) and 30% weight loss (T_{d30}) were listed in Table II. In order to make a quantitative comparison of thermal stability, the statistic heat-resistant index (T_s) determined by the following equation was applied eq. (5)[33]:

$$T_s = 0.49[T_{d5} + 0.6(T_{d30} - T_{d5})] \quad (5)$$

The calculated T_s were also listed in Table II. The thermal degradation behaviors were similar to each other, which were also comparable to those of DER331 cured by the petroleum-based counterparts.

CONCLUSIONS

Two kinds of biobased curing agents were prepared from rosin acid and isosorbide to serve as alternatives to petroleum-based rigid curing agents. The results indicated that, compared with TAR, RSR was more effective in improving the thermal properties of the cured resin. The DER331 cured with bio-based curing agents (RSR and ISR) possessed higher shape fixity and recovery as well as better shape memory cyclic performance. The diverse ring structures in the curing agents have significant effects on the properties of the cured resins, especially the shape memory properties.

ACKNOWLEDGMENTS

The authors are grateful for the financial support from National Natural Science Foundation of China (NSFC No. 51373194; NSFC No. 51203176), Youth Innovation Promotion Association of the Chinese Academy of Sciences (2012229) and Natural Sciences Foundation of Ningbo City (No. 2014A610110).

REFERENCES

1. Luo, X.; Mather, P. T. *Soft Matter* **2010**, *6*, 2146.
2. Shi, Y.; Yoonessi, M.; Weiss, R. A. *Macromolecules* **2013**, *46*, 4160.

3. Chen, S.; Hu, J.; Yuen, C. W.; Chan, L. *Polymer* **2009**, *50*, 4424.
4. Andreas, L.; Hongyan, J.; Oliver, J.; Robert, L. *Nature* **2005**, *434*, 879.
5. Li, Y.; Chen, H. M.; Liu, D.; Wang, W. X.; Liu, Y.; Zhou, S. B. *ACS Appl. Mater. Interface* **2015**, *7*, 12988.
6. Razzaq, M. Y.; Behl, M.; Kratz, K.; Lendlein, A. *Adv. Mater.* **2013**, *25*, 5730.
7. Rousseau, I. A. *Polym. Eng. Sci.* **2008**, *48*, 2075.
8. Leonardi, A. B.; Fasce, L. A.; Zucchi, I. A.; Hoppe, C. E.; Soulé, E. R.; Pérez, C. J.; Williams, R. J. J. *Eur. Polym. J.* **2011**, *47*, 362.
9. Rousseau, I. A.; Xie, T. *J. Mater. Chem.* **2010**, *20*, 3431.
10. Wu, X.; Yang, X.; Zhang, Y.; Huang, W. *J. Mater. Sci.* **2016**, *51*, 3231.
11. Brogly, M.; Fahs, A.; Bistac, S. *Key Eng. Mater.* **2014**, *611-612*, 829.
12. Cheng, D.; Matharu, A. S. *ACS Sustain. Chem. Eng.* **2014**, *2*, 2217.
13. Ma, Q.; Liu, X.; Zhang, R.; Zhu, J.; Jiang, Y. *Green Chem.* **2013**, *15*, 1300.
14. Chrysanthos, M.; Galy, J.; Pascault, J. P. *Polymer* **2011**, *52*, 3611.
15. Feng, X.; East, A. J.; Hammond, W. B.; Zhang, Y.; Jaffe, M. *Polym. Adv. Technol.* **2011**, *22*, 139.
16. Goerz, O.; Ritter, H. *Polym. Int.* **2013**, *62*, 709.
17. Liu, X.; Xin, W.; Zhang, J. *Bioresour. Technol.* **2010**, *101*, 2520.
18. Ma, S.; Liu, X.; Jiang, Y.; Tang, Z.; Zhang, C.; Zhu, J. *Green Chem.* **2013**, *15*, 245.
19. Stemmelen, M.; Pessel, F.; Lapinte, V.; Caillol, S.; Habas, J. P.; Robin, J. J. *J. Polym. Sci., Part A: Polym. Chem.* **2011**, *49*, 2434.
20. Chang, R.; Qin, J.; Gao, J. *J. Polym. Res.* **2014**, *21*, 1.
21. Ma, S.; Liu, X.; Fan, L.; Jiang, Y.; Cao, L.; Tang, Z. *ChemSusChem* **2014**, *7*, 555.
22. Takashi, T.; Takeshi, T.; Hiroshi, U. *Polymers* **2015**, *7*, 2165.
23. Remi, A.; Sylvain, C.; Ghislain, D.; Bernard, B.; Jean, P. *Chem. Rev.* **2014**, *114*, 1082.
24. Xie, T.; Rousseau, I. A. *Polymer* **2009**, *50*, 1852.
25. Zhang, L. S.; Jiang, Y. H.; Xiong, Z.; Liu, X. Q.; Na, H. N.; Zhang, R.; Zhu, J. *J. Mater. Chem. A* **2013**, *1*, 3263.
26. Li, C.; Dai, J. Y.; Liu, X. Q.; Jiang, Y. H.; Ma, S. Q.; Zhu, J. *Macromol. Chem. Phys.* **2016**, *217*, 1439.
27. Liu, Y.; Han, C.; Tan, H.; Du, X. *Mater. Sci. Eng. A* **2010**, *527*, 2510.
28. Liu, W. B.; Qiu, Q. H.; Wang, J.; Huo, Z. C.; Sun, H. *Polymer* **2008**, *49*, 4399.
29. Kissinger, H. E. *J. Res. Natl. Bur. Stand.* **1956**, *57*, 217.
30. Ozawa, T. *J. Therm. Anal.* **1976**, *9*, 369.
31. Wei, K.; Zhu, G. M.; Tang, Y. S.; Tian, G. M.; Xie, J. Q. *Smart Mater. Struct.* **2012**, *21*, 55022.
32. Wei, K.; Zhu, G. M.; Tang, Y. S.; Li, M. M.; Liu, T. T. *Smart Mater. Struct.* **2012**, *21*, 85016.
33. Qin, J.; Liu, H.; Zhang, P.; Wolcott, M.; Zhang, J. *Polym. Int.* **2014**, *63*, 760.